+ Model
ARTICLE IN PRESS
Available online at www.sciencedirect.com
SCIENCE DIRECT
ELSEVIER
Electric Power Systems Research xxx (2005) xxx–xxx
ELECTRIC POWER SYSTEMS RESEARCH
www.elsevier.com/locate/epsr

Fault analysis of Korean AC electric railway system

Hanmin Lee [a,b], Gildong Kim [a], Sehchan Oh [a], Gilsoo Jang [b,*], Sae-hyuk Kwon [b]

[a] *Korea Railroad Research Institute, #374-1, Woulam-Dong, Uiwang-City, Kyunggi-do 437-050, South Korea*
[b] *Department of Electrical Engineering, Korea University, 5-1 Anam-dong, Sungbuk-gu, Seoul 136-701, South Korea*

Received 28 May 2005; accepted 3 August 2005

Abstract

This paper presents the fault analysis of Korean AC electric railway system. The AC electric railway system is modeled by PSCAD/EMTDC tool. This system model is composed of the Scott-transformer, the autotransformer, the running rails, the protection wires, the feeders, messenger wires and contact wires, etc. After obtaining the models of the fundamental elements describing Korean AC electric railway system, studies for the steady state and fault conditions are carried out. Simulation result and hand calculation for the fault analysis are compared with field data. Finally, we acquire the specific characteristic of Korean AC electric railway system. The proposed model would be a powerful tool for designing and planning Korean AC electric railway system.

Keywords: Fault analysis; PSCAD/EMTDC; Korean AC electric railway system

1. Introduction

An electric railway system has a number of advantages in terms of traffic capability, energy efficiency, operational cost and environmental friendliness in comparison with other transportation systems. Nonetheless, it still has matters of unexpected fault occurrence threatening safety of passengers or electrical and signal equipments.

If the fault is occurred in an AC electric railway system, it should be quickly eliminated and distinguished for normal operation on the safe aspect. It is required to carry out a careful study on the fault occurrence when an AC electric railway system is designed and planned. Therefore, it is important to model Korean AC electric railway system for fault studies. This system is composed of each individual subsystem such as the power supply network, the catenary system, the autotransformer, etc. So, this paper models each individual subsystem using PSCAD/EMTDC simulation software [1].

In order to verify the proposed model, studies for fault current are carried out. Simulation results are compared with field data and hand calculations to obtain an acceptable accuracy for the integrated model of all constituent subsystems.

2. Korea AC electric railway system

The AC electric railway system in Korea is based on single-phase 55/27.5 kV. AC feeding circuits supply electric trains with the electric power through three-phase to two-phase Scott-transformers, feeders, contact wires and rails. Autotransformers are installed approximately every 10 km with circuit breakers which connect adjacent up and down tracks at the parallel post (PP). Substations (SS) are located about every 50 km away, and a sectioning post (SP) is between two substations. The SP has circuit breakers, which enable one feeding circuit to electrically separate from the other. They may be closed, in case the adjacent SS is out of service [2–4]. Fig. 1 shows a typical AC electric railway system.

Fig. 2 is the representation of Korea AC electric railway system made by PSCAD/EMTDC, and it includes each subsystem module.

To analyze Korean AC electric railway system for the steady state and fault conditions, modeling for each railway system is performed as eight-port network model that is an extension of two-port network theory [5]. The modeling is performed for the power supply, the autotransformer, the catenary system. Korean AC electric railway system is composed by the common grounding system, which means rails on up/down track, protection wires on up/down track and grounding conductors are connected commonly. The overall conductors are reduced as equivalent five

* Corresponding author. Tel.: +82 2 3290 3246; fax: +82 2 3290 3692.
E-mail address: gjang@korea.ac.kr (G. Jang).

0378-7796/$ – see front matter © 2005 Elsevier B.V. All rights reserved.
doi:10.1016/j.epsr.2005.08.001

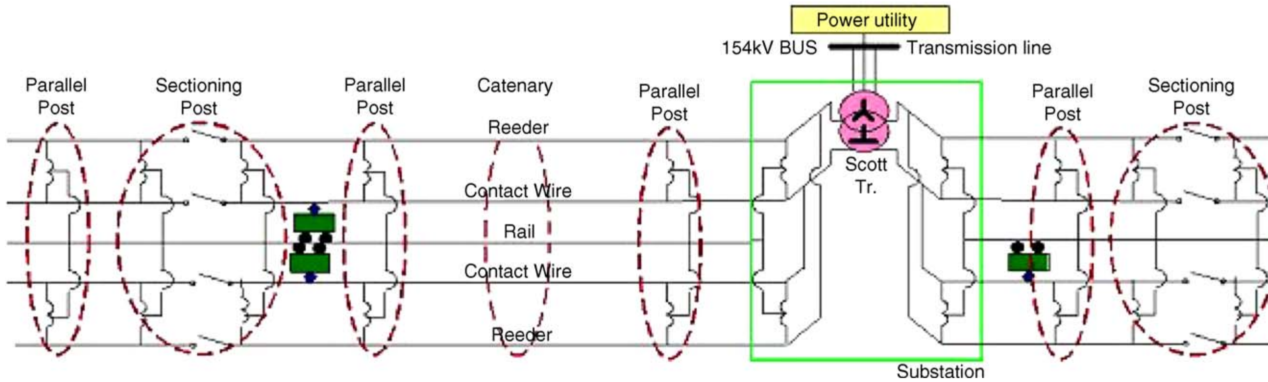

Fig. 1. Korean AC electric railway system.

conductors electrically. The railway system is expressed by port network model. In this paper, Korean AC electric railway system is modeled by eight-port representation. Eight-port representation means that the system has four input ports, four output ports and a basic port. Namely, there are input/output port of feeder on up/down track, input/output port of contact wire group on up/down track, input/output port of rail group. Finally, the entire system can be easily modeled by the combination of eight-port representation of each component in parallel and/or series.

2.1. Power supply

As in Fig. 3, power utility, Korea Electric Power Corporation (KEPCO), supplies 154 kV with the AC electric railway system. Scott-transformers in the substation transform 154 into 55 kV. Two pairs of single-phase power are obtained from Scott-transformers. The turn ratios of T phase and M phase are $\sqrt{3}/2N_1:N_2$ and $N_1:N_2$, respectively.

The connection diagram of a Scott-transformer appears in Fig. 4.

2.2. Autotransformer

An autotransformer is placed between the catenary and the adjacent feeder, and the rail is connected to the center point of the winding. The AC electric railway system supplies 55 kV between the contact wire and the feeder with the autotransformer of ratio l:l (feeder-rail:rail-contact wire) to step down the high voltage 55–27.5 kV. Autotransformers are installed approximately every 10 km along the railway. The equivalent circuit of the autotransformer is presented in Fig. 5.

The catenary system has several conductors with a complex geometry, and the geometry is shown in Fig. 6. The system consists of contact wires (4, 6), messenger wires (3, 5), feeders (1, 2), rails (7–10), protection wires (11, 12) and buried earth wires (13, 14). Droppers connect two conductors such as the contact wire and the messenger wire. Those conductors are electrically regarded as one conductor. This simplification is made possible by the continuous parallel connection of some conductors. Finally, we can reduce the overall conductors to the equivalent of five conductors [6,7].

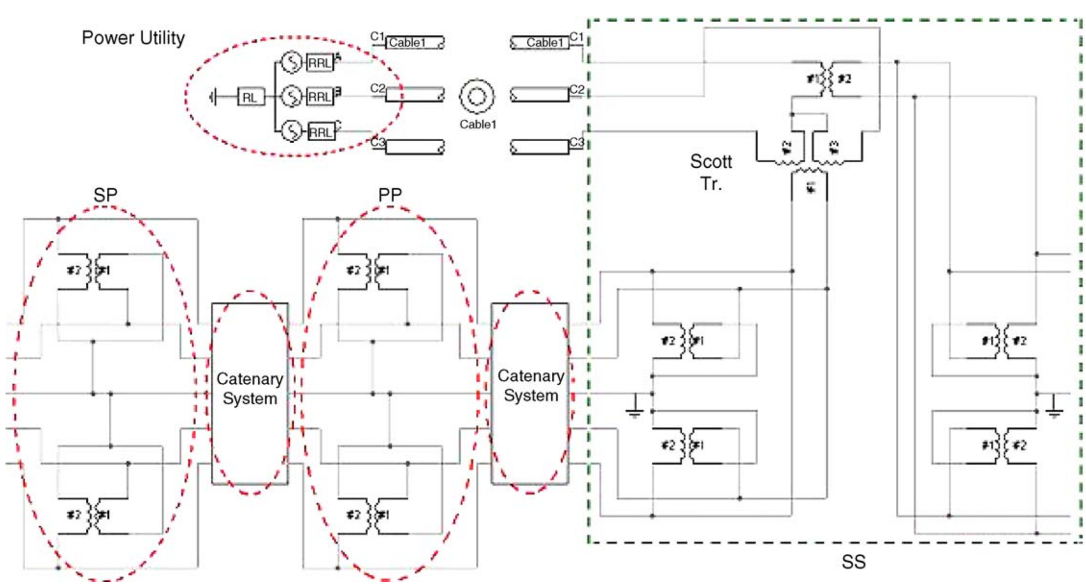

Fig. 2. Model of Korean AC electric railway system made by PSCAD/EMTDC.

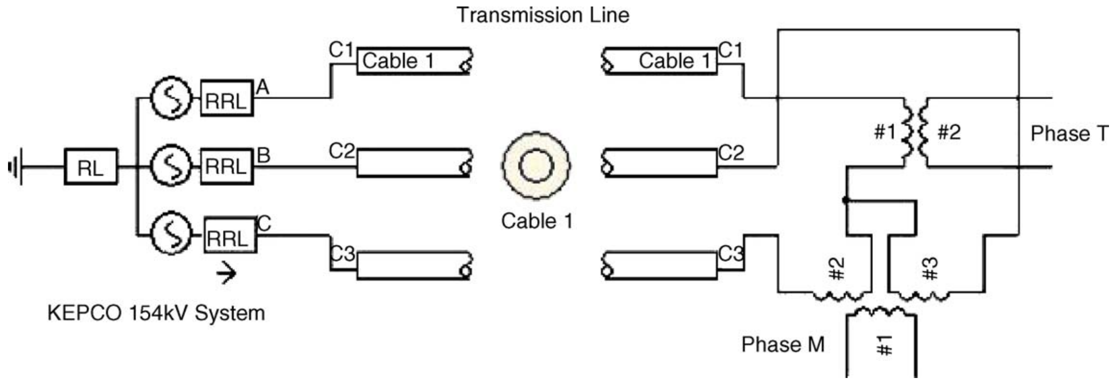

Fig. 3. Power utility, transmission line and Scott-transformer.

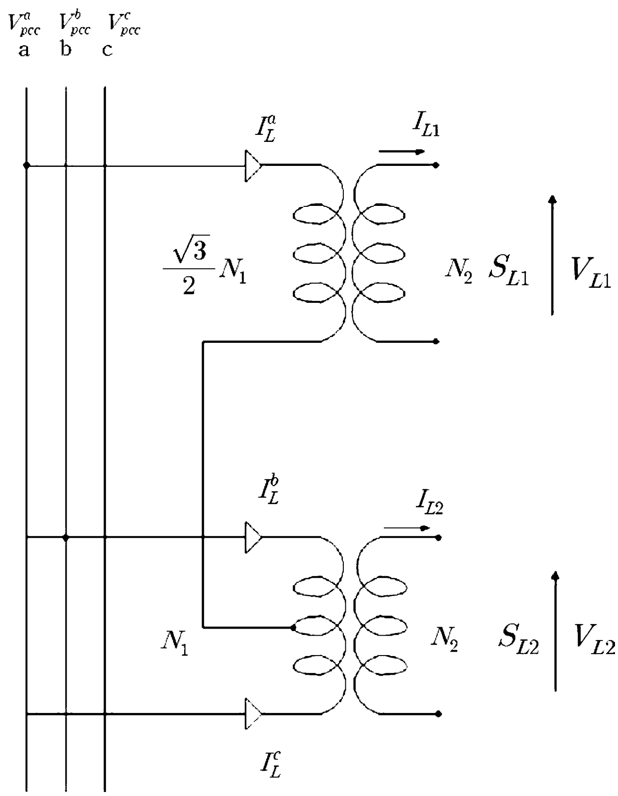

Fig. 4. Scott-transformer.

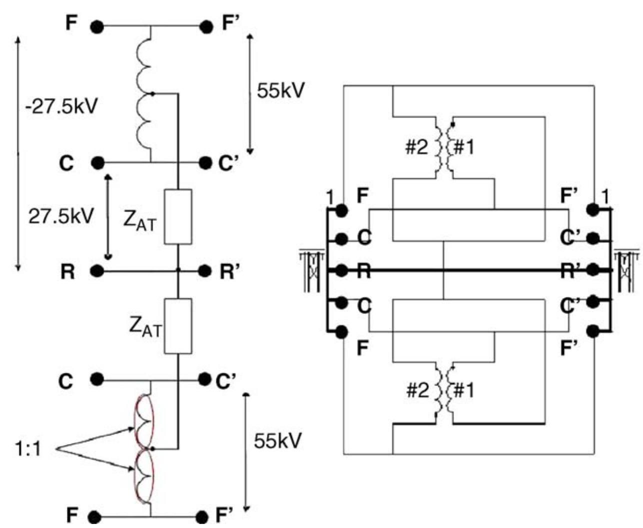

Fig. 5. Autotransformer.

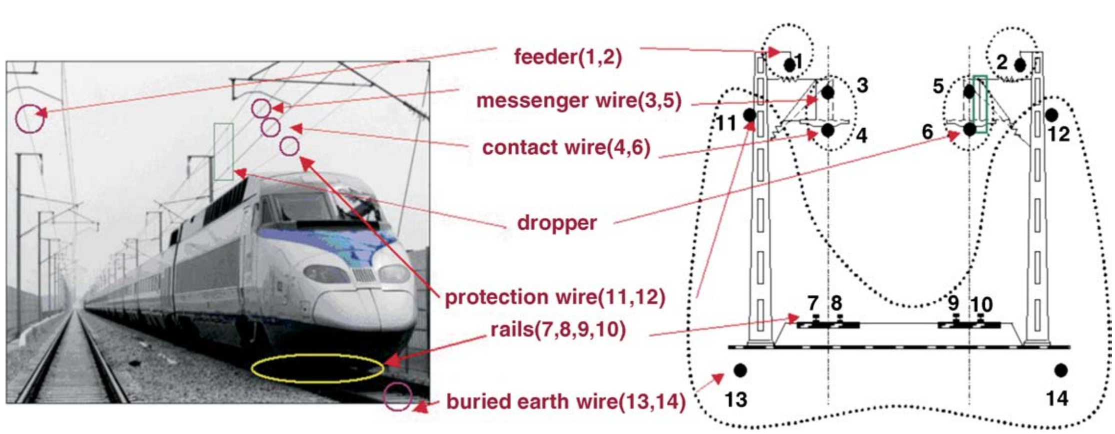

Fig. 6. Configuration of the catenary system.

All values for self and mutual impedances are evaluated by the Carson equations. The equivalent five conductors are calculated by the reduction method. The reduced system is composed by PSCAD/EMTDC.

3. Case study

3.1. Designing system

3.1.1. Power supply

- 154[kV] bus impedance of power utility

$$\%Z_{S1} = 0.0875 + j1.3708 \quad (100[\text{MVA}]\text{Base})$$
$$\%Z_{S2} = 0.0875 + j1.3708 \quad (100[\text{MVA}]\text{Base})$$
$$\%Z_{S0} = 0.2450 + j1.9267 \quad (100[\text{MVA}]\text{Base})$$

$$Z_{S1} = 0.2075 + j3.2510[\Omega] \quad (154[\text{kV}], 3[\Phi]\text{Base})$$
$$Z_{S2} = 0.2075 + j3.2510[\Omega] \quad (154[\text{kV}], 3[\Phi]\text{Base})$$
$$Z_{S0} = 0.5810 + j4.5694[\Omega] \quad (154[\text{kV}], 3[\Phi]\text{Base})$$

$$Z_{S1} = 0.0132 + j0.2073[\Omega] \quad (27.5[\text{kV}], 1[\Phi]\text{Base})$$
$$Z_{S2} = 0.0132 + j0.2073[\Omega] \quad (27.5[\text{kV}], 1[\Phi]\text{Base})$$
$$Z_{S0} = 0.0371 + j0.2990[\Omega] \quad (27.5[\text{kV}], 1[\Phi]\text{Base})$$

3.1.2. Transmission line

- Cable: XLPE 400[mm^2], 4.0[km]

$$Z_{T1} = (0.09127 + j0.14005) \times 4.0 = 0.3651 + j0.562[\Omega]$$
$$Z_{T0} = (0.11025 + j0.11857) \times 4.0 = 0.441 + j0.4743[\Omega]$$

$$\%Z_{T1} = \%Z_{T2} = 0.1539 + j0.237[\%] \quad (100[\text{MVA}]\text{Base})$$
$$\%Z_{T0} = 0.186 + j0.2[\%] \quad (100[\text{MVA}]\text{Base})$$

$$Z_{T1} = 0.0233 + j0.0358[\Omega] \quad (27.5[\text{kV}], 1[\Phi]\text{Base})$$
$$Z_{T0} = 0.0281 + j0.0303[\Omega] \quad (27.5[\text{kV}], 1[\Phi]\text{Base})$$

3.1.3. Scott-transformer

$$\frac{40[\text{MVA}],}{50[\text{MVA}],} \quad \frac{154[\text{kV}]}{55[\text{kV}]} \times 2, \quad \%Z = 10, \quad \frac{X}{R} = 20$$
(IEEE STD 141, 1976, Page 201, Fig. 77)

$$\%Z_{\text{Tr}} = 0.4993 + j9.9875[\%] \quad (15[\text{MVA}]\text{Base})$$
$$\%Z_{\text{Tr}} = 3.3286 + j66.583[\%] \quad (100[\text{MVA}]\text{Base})$$

$$Z_{\text{Tr}} = 0.2517 + j5.0353[\Omega] \quad (27.5[\text{kV}], 1[\Phi]\text{Base})$$
$$Z_{\text{Tr}} = 7.8942 + j157.9090[\Omega] \quad (154[\text{kV}], 3[\Phi]\text{Base})$$

3.1.4. Autotransformer

$$1000[\text{kVA}], \quad Z_{\text{AT}} = 0.45[\Omega] \quad (27.5[\text{kVA}]\text{Base}),$$
$$\frac{X}{R} = 14 \quad (\text{IEEE STD 141, 1976, Page 201, Fig. 77})$$

$$Z_{\text{AT}} = 0.0320 + j0.4488[\Omega]$$

4. Steady state analysis

The Scott-transformer steps down 154 (N_1) to 55 kV (N_2). Two pairs of single-phase power is obtained from the Scott-transformer. The accuracy of the Scott-transformer model is confirmed by voltage and angle difference of M phase and T phase. T phase leads M phase by 90° as shown in Fig. 7.

No-load voltages between each conductor are shown in Fig. 8. The secondary voltage of the Scott-transformer is 55 kV and

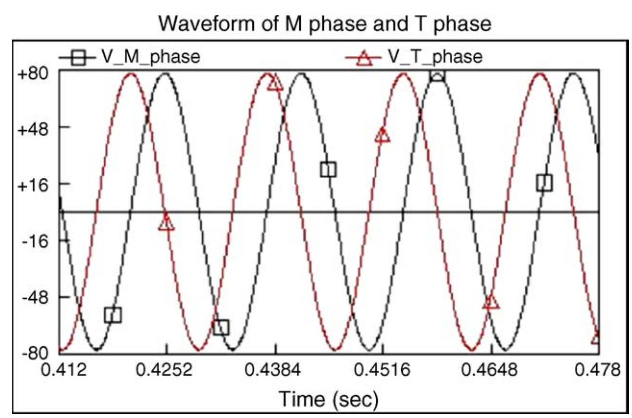

Fig. 7. Voltage and angle difference of M phase and T phase.

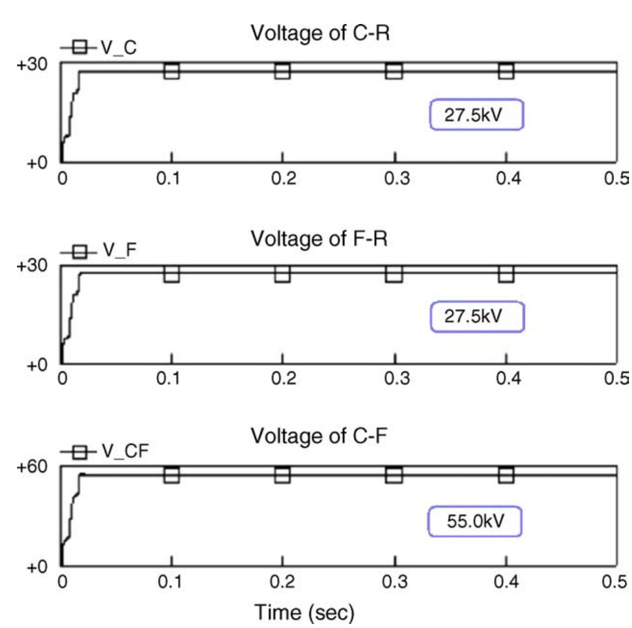

Fig. 8. Voltages between each conductor in no-load condition.

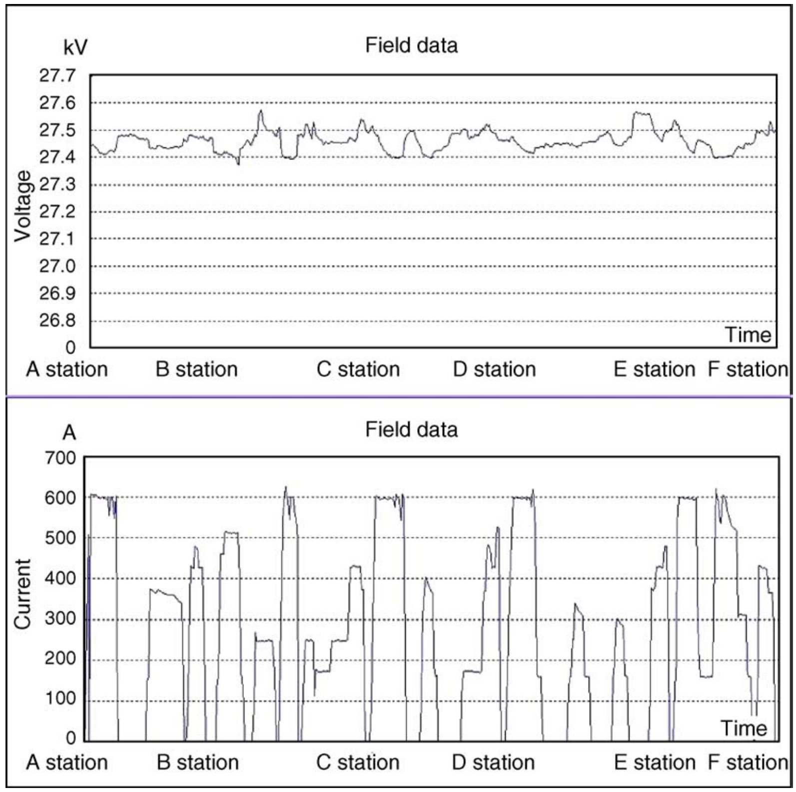

Fig. 9. Voltage and current in substation measured from field.

the secondary voltages of the autotransformer, i.e. voltages of contact wire-to-rail (C-R), feeder-to-rail (F-R) and contact wire-to-feeder (C-F), are 27.5, 27.5 and 55 kV, respectively.

We have observed the secondary voltage of the Scott-transformer under no-load condition and secondary voltages of the autotransformer.

The electric train is modeled by field voltage and current. This model represents the moving characteristics of the electric train that are starting, acceleration and breaking.

This load reads measured voltage and current from field and outputs them. The voltage and current in the substation are also measured from field. Those data are shown in Fig. 9.

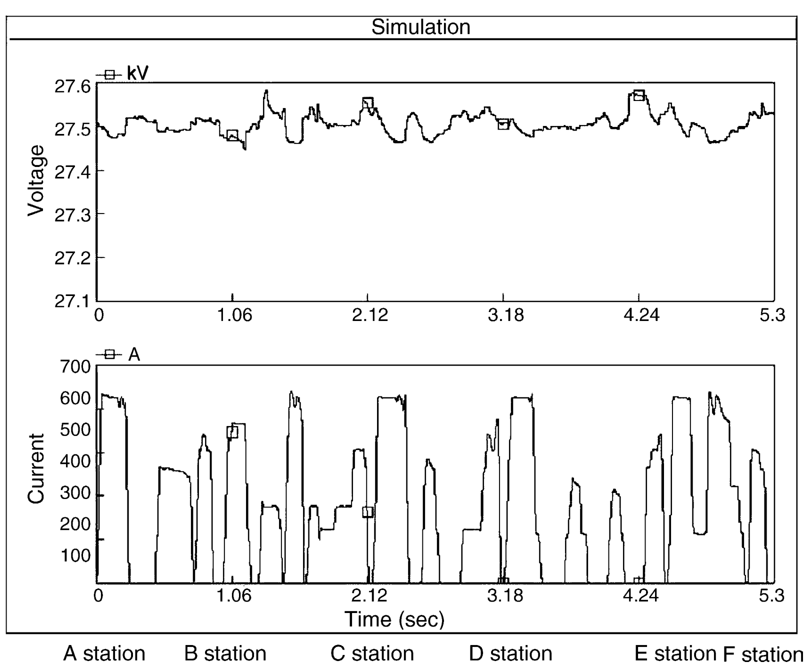

Fig. 10. Voltage and current in substation simulated by PSCAD/EMTDC.

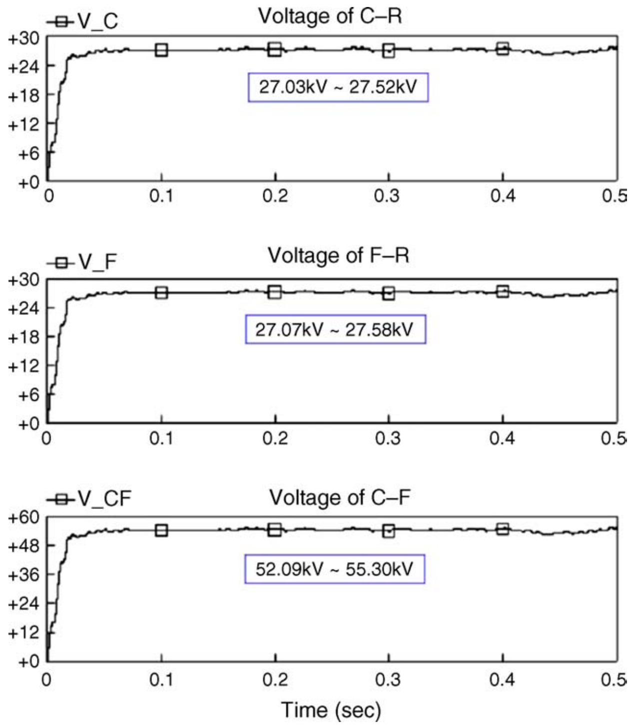

Fig. 11. Voltages between each conductor in load condition.

The results simulated by PSCAD/EMTDC are shown in Fig. 10. It presents the same result as voltage and current measured from field.

The voltages between each conductor are shown in Fig. 11. Unlike no-load condition, voltages are slightly varied by electric train because of its power consumption and regeneration.

5. Fault analysis

5.1. 154[kV] single phase-to-ground

- Diagram

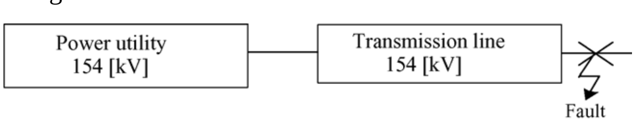

- Calculation

Zero-sequence

	R	X	
Power utility 154[kV]	0.58 10	4.5694	Series
Transmission line 154[kV]	0.44 10	0.4743	
Total	1.0220	5.0437	

Positive-sequence

	RX		
Power utility 154 [kV]	0.2075	3.2510	Series
Transmission line 154 [kV]	0.3651	0.5620	
Total	0.57263.8	130	

Negative-sequence

	RX		
Power utility 154 [kV]	0.2075	3.2510	Series
Transmission line 154 [kV]	0.3651	0.5620	
Total	0.57263.8	130	

$$Z_0 = 1.0220 + j5.0437[\Omega]$$
$$Z_1 = 0.5726 + j3.8130[\Omega]$$
$$Z_2 = 0.5726 + j3.8130[\Omega]$$
$$Z_0 + Z_1 + Z_2 = 2.1672 + j12.6730[\Omega]$$
$$Z_{SF} = \sqrt{2.1672^2 + 12.6730^2} = 12.857[\Omega]$$

- Fault current

$$I_g = \frac{3E}{Z_0 + Z_1 + Z_2} = \frac{3}{12.857} \times \frac{154,000}{\sqrt{3}} = 20.746[\text{kA}]$$

5.2. 154[kV] three phase-to-ground

- Diagram

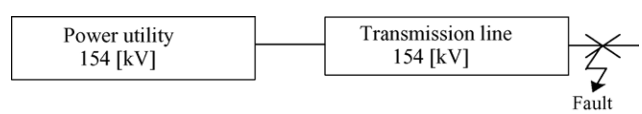

- Calculation

	RX		
Power utility 154 [kV]	0.0875	1.3708	Series
Transmission line 154 [kV]	0.1539	0.2369	
Total	0.2414	1.6077	

$$\%Z_{SF} = \sqrt{0.2414^2 + 1.6077^2} = 1.6257[\%]$$

- Fault current

$$P_S = \frac{100 P_n}{\%Z_{SF}} = \frac{100 \times 100}{1.6257} = 6.15[\%]$$
$$I_{S1} = \frac{P_3}{\sqrt{3}V} = \frac{6.151}{\sqrt{3 \times 154}} = 23.06[\text{kA}]$$

5.3. 55[kV] phase-to-phase

- Diagram

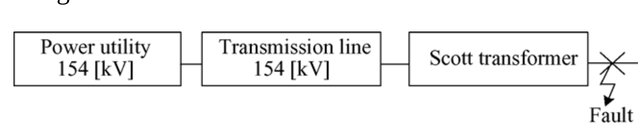

- Calculation

	R	X	
Power utility 154 [kV]	0.0132	0.2073	Series
Transmission line 154 [kV]	0.0233	0.0358	
Scott transformaer (M-phase)	0.2517	5.0353	
Total	0.28825.2784		

$$Z_{SF} = \sqrt{0.2882^2 + 5.2784^2} = 5.2863[\Omega]$$

- Fault current

$$I_{SF} = \frac{E}{Z_{SF}} = \frac{27,500}{5.2863} = 5.202[\text{kA}] \quad (27.5[\text{kV}]\text{Base})$$

$$I_{SF} = \frac{5.202}{2} = 2.6[\text{kA}] \quad (55[\text{kV}]\text{Base})$$

5.4. 27.5[kV] single phase-to-ground

- Diagram

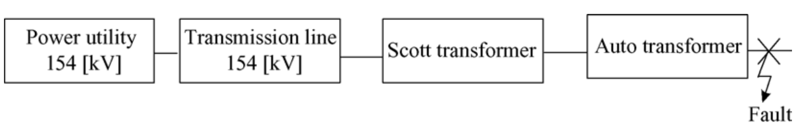

- Calculation

	R	X	
Power utility 154 [kV]	0.0 132	0.2073	Series
Transmission line 154 [kV]	0.0233	0.0358	
Scott transformaer (M-phase)	0.25 17	5.0353	
Auto-transformer	0.0320	0.4488	
Total	0.3302	5.7272	

$$Z_{SF} = \sqrt{0.3202^2 + 5.7272^2} = 5.736[\Omega]$$

- Fault current

$$I_{SF} = \frac{E}{Z_{SF}} = \frac{27,500}{5.7361} = 4.794[\text{kA}] \quad (27.5[\text{KV}]\text{Base})$$

6. PSCAD/EMTDC simulation

Simulation conditions are even as Section 3.1. To compare hand calculations with PSCAD/EMTDC simulation results, results are shown in Table 1 and Fig. 12.

Results of hand calculation and simulation are almost same. The difference is because the catenary system, parallel post and sectioning post as well as substation are composed by the continuous parallel connection in model. Because impedances of system simulated by PSCAD/EMTDC are lower than those in hand calculations, fault currents in simulation are higher than those in hand calculations.

Table 1
Comparison of fault currents for each case

	Fault current	
	PSCAD/EMTDC (kA)	Hand calculation (kA)
154 kV single phase-to-ground	22.00	20.75
154 kV three phase-to-ground	23.56	23.06
55 kV phase-to-phase	3.12	2.60
27.5 kV single phase-to-ground	5.36	4.79

The simulation model is easy to use, flexible, efficient and accurate modeling of all components. Furthermore, we simulate various fault studies, assuming faults are occurred every 2 km.

Types of fault are listed:

- contact wire-to-rail;
- feeder-to-rail;
- contact wire-to-feeder.

The fault current measured at the fault location are shown in Figs. 13 and 14.

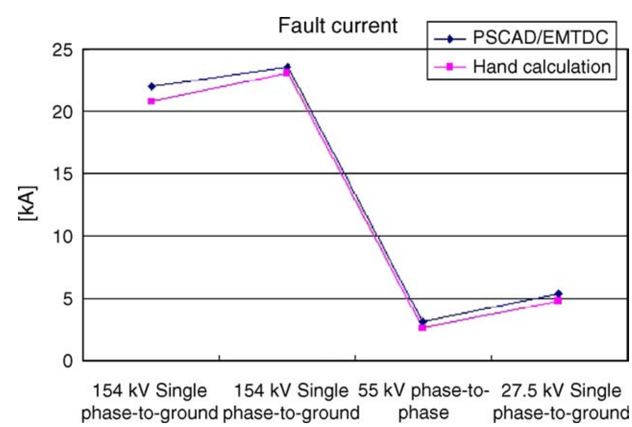

Fig. 12. Comparison of fault currents simulated by PSCAD/EMTDC and hand calculation.

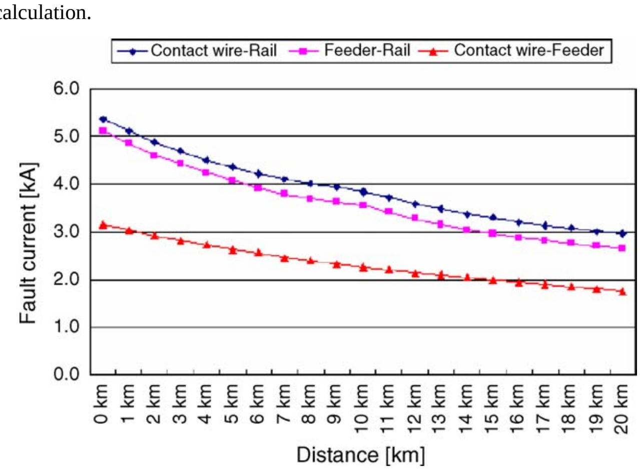

Fig. 13. Comparison of fault currents simulated by PSCAD/EMTDC.

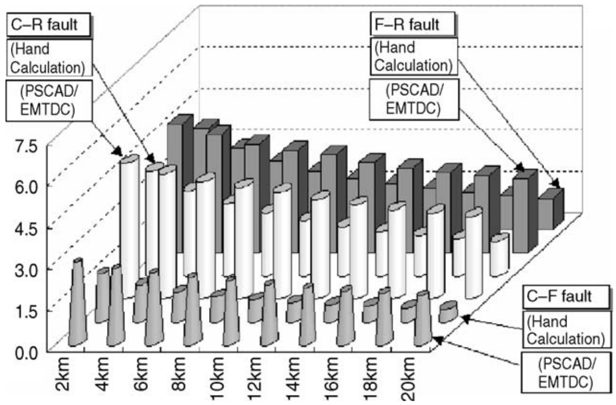

Fig. 14. Comparison of fault currents by simulation and hand calculation according to locations and fault types.

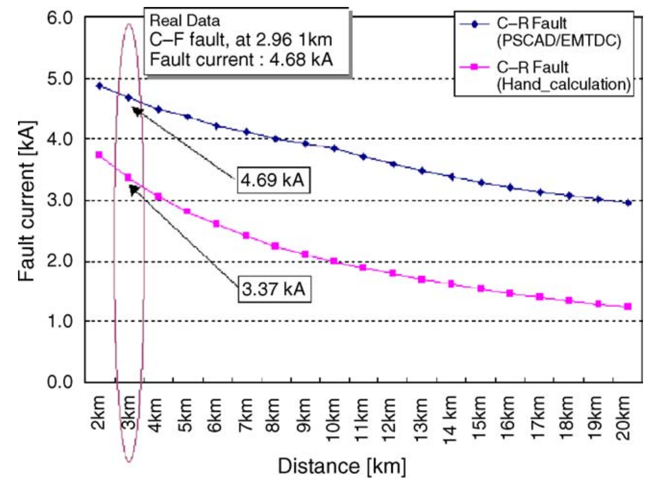

Fig. 16. Comparison of C-R fault currents simulated by PSCAD/EMTDC and hand calculation.

In case of C-F fault, fault currents are relatively lower because the voltage level is higher than that of C-R (or F-R). As the simulation shown in Fig. 13, fault currents describe a parabola. The impedance of the catenary system is that the characteristic increased with describing a parabola, not a straight line. Results of simulation and hand calculation are different as shown in Fig. 14, because such a characteristic of impedance is considered in simulation. The fault current rises at the point that the autotransformer is installed. The impedance gets higher at the middle point of two autotransformers (PP-PP or PP-SP) and lower at the autotransformer. So, the fault current rises at the point of the autotransformer (PP or SP), which is located at 10 km (or 20 km). Because the voltage level of C-F is higher than that of C-R (or F-R). The fault current of C-F is lower, respectively.

In real system, a C-R fault was occurred at 2.961 km as shown in Fig. 15. The fault current was 4.68 kA. While the result of hand calculation is 3.37 kA, the simulation result of fault current is 4.69 kA at 3 km as shown in Fig. 16.

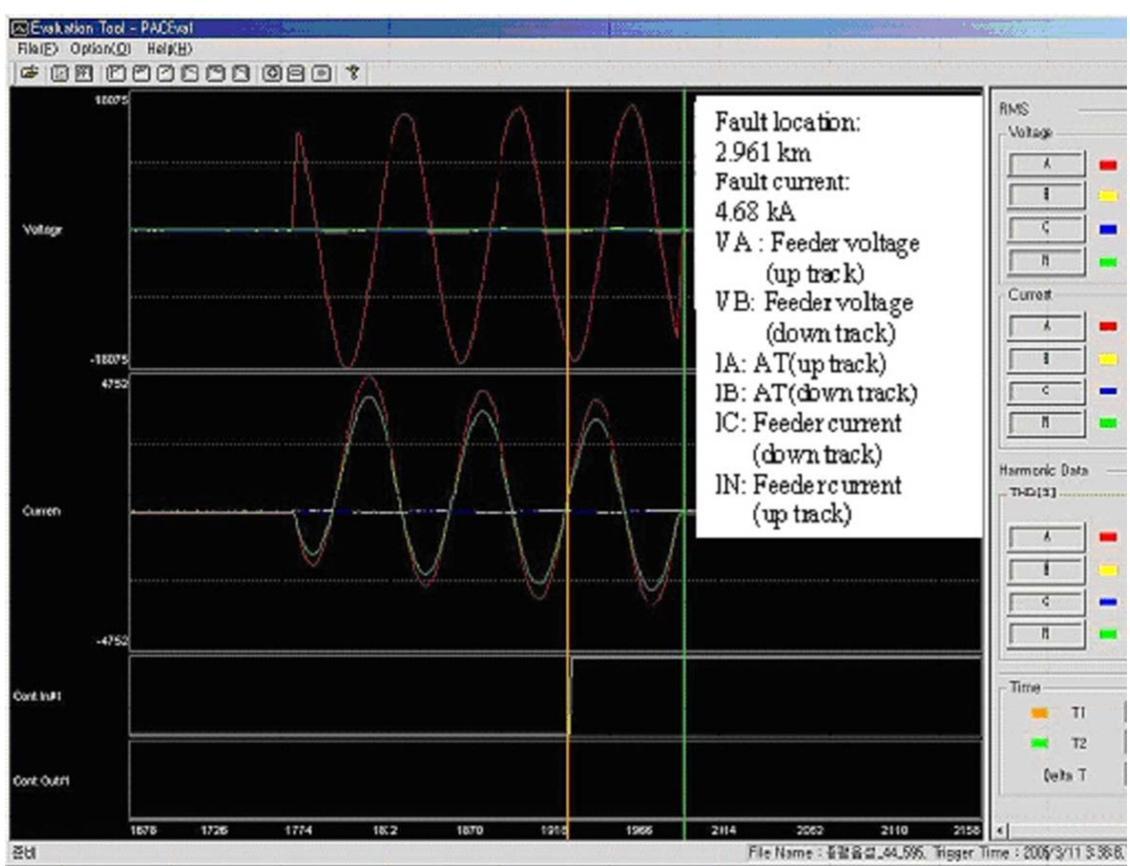

Fig. 15. Measured C-R fault current.

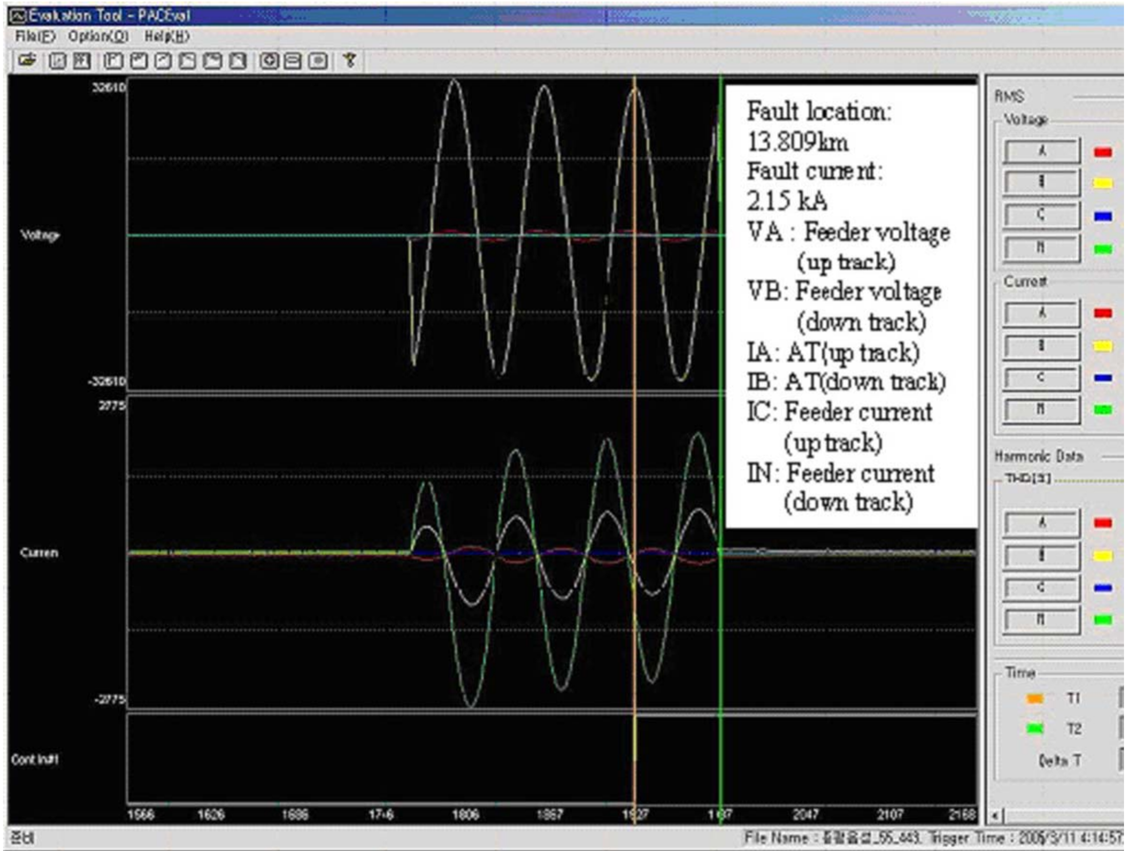

Fig. 17. Measured C-F fault current.

As shown in Fig. 17, similarly, a C-R fault was occurred at 13.809 km. The fault current was 2.15 kA. While the result of hand calculation is 0.62 kA, the simulation result of fault current is 2.03 kA at 14 km as shown in Fig. 18.

In real system, a fault is not often occurred. Results of two cases are compared. From the results, we can observe the simulation model reflects more precisely the characteristics of Korean AC electric railway system.

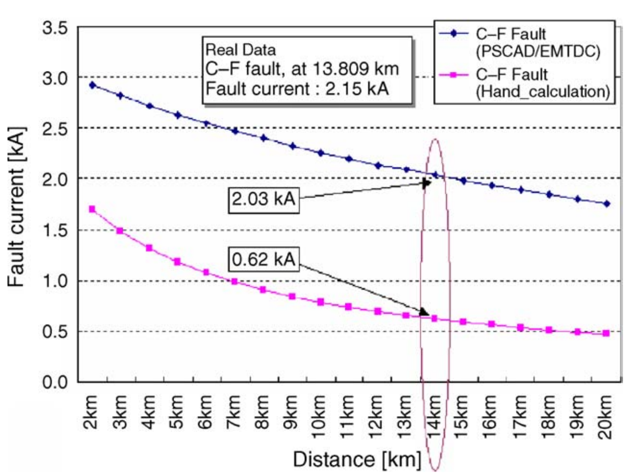

Fig. 18. Comparison of C-F fault currents simulated by PSCAD/EMTDC and hand calculation.

7. Conclusion

This paper presents analysis model for fault studies using PSCAD/EMTDC. This system is composed of integrating all constituent subsystems. To verify the proposed model, simulation results are compared with hand calculations and field data.

The impedance of the catenary system has the characteristic increased with describing a parabola, not a straight line. Hence, the fault currents also follow a parabola. There is a difference between hand calculation and field data, because such a characteristic of impedance cannot be considered in hand calculation. This can be a reason why the model using PSCAD/EMTDC is needed.

From results of field data, we can observe the result of simulation using PSCAD/EMTDC is more accurate than that of hand calculation because it well reflects the characteristic of Korean AC electric railway system.

Furthermore, the advantage of using the PSCAD/EMTDC model is as follows:

(1) it is easy to use, flexible and efficient;
(2) accurate modeling of all components is possible;
(3) repeated simulations are possible;
(4) impedance and shunt admittances for catenary system can be considered;
(5) train's moving model according to the train schedules can be simulated.

The proposed model would be a powerful tool for designing and planning Korean AC electric railway system modeled by eight-port representation, and it will be applied to perform a more precise analysis including determination of fault types, positions and locations.

References

[1] P. Wilson, PSCAD USER'S GUIDE, RESEARCH CENTRE, Canada, 2003.
[2] K.H. Oh, H.M. Lee, S.H. Chang, Harmonic analysis model based on 8-port representation for Korean high speed railway, November 25–29, Cologne, Germany WCRR, 2001.
[3] H.M. Lee, C.M. Lee, H.S. Cho, G.S. Jang, S.H. Kwon, Harmonic Analysis Model based on PSCAD/EMTDC for Korean High-Speed Railway 2004 Large Engineering Systems Conference on Power Engineering, July 5–6, Japan, 2004, pp. 93–97.
[4] N.J. Balu, Railroad electrification on utility system, EPRI, EL-3001, Contract TPS 81-796, 1983, pp. 60–83.
[5] S.H. Chang, K.H. Oh, J.H. Kim, Analysis of voltage unbalance in the electric railway depot using two-port network model, in: International Conference on Electrical Engineering, August 6–10, Oslo/Bergen, Norway, 2001, pp. 852–858.
[6] P. Ferrari, P. Pozzobon, Railway lines models for impedance evaluation, in: Eighth International Conference on Harmonics and Quality of Power ICHQP'98, October 14–16, Athens, Greece, 1998, pp. 641–646.
[7] International Telecommunication Union, Directives concerning the protection of telecommunication lines against harmful effects from electric power and electrified railway lines, vol. V, CCITTT, 1989.